International Conference on Space Optics—ICSO 2020

Virtual Conference

30 March–2 April 2021

Edited by Bruno Cugny, Zoran Sodnik, and Nikos Karafolas

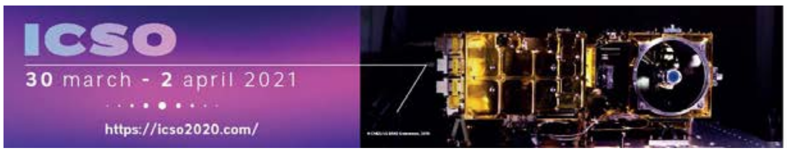

Proton radiation assessment of COTS components of 100 Gb/s digital coherent transceiver for optical satellite communications

International Conference on Space Optics — ICSO 2020, edited by Bruno Cugny, Zoran Sodnik, Nikos Karafolas, Proc. of SPIE Vol. 11852, 118525I · © 2021 ESA and CNES
CCC code: 0277-786X/21/$21 · doi: 10.1117/12.2599961

Proton Radiation Assessment of COTS Components of 100 Gb/s Digital Coherent Transceiver for Optical Satellite Communications

Keisuke Matsuda*[a], Yuzo Yajima[b], Shun Chikamori[a], Shota Koshikawa[a], Tsuyoshi Yoshida[a] and Naoki Suzuki[a]
[a]Information Technology R&D Center, Mitsubishi Electric Corporation, 5-1-1 Ofuna, Kamakura, Kanagawa 247-8501, Japan; [b] Kamakura Works, Mitsubishi Electric Corporation, 325 Kamimachiya, Kamakura, Kanagawa, 247-8520, Japan

ABSTRACT

Digital coherent detection and wavelength division multiplexing are promising technologies for achieving throughputs from 100 Gb/s to Tb/s order in optical satellite communications. The adoption of these technologies leads to the possibility of using high performance, low cost commercial off the shelf (COTS) components for satellite communications. In this paper, as COTS optical devices and a DSP-ASIC suitable for enabling 100 Gb/s/wavelength capacity, a micro integrable tunable laser assembly, a lithium niobate modulator, a micro intradyne coherent receiver (Micro ICR) and a DSP-ASIC for 100 Gb/s fiber optical communications were successively exposed to a total fluence of more than 4.0×10^{10} p/cm^2 of 70 MeV protons. This fluence is equivalent to the total non-ionizing dose (TNID) and total ionizing dose (TID) experienced during 10 years in low earth orbit. The components were powered, and the performance of a 100 Gb/s signal was measured during irradiation to assess the single event effect (SEE). All components showed no degradation as a result of TNID/TID effects. On the other hand, the Micro ICR and DSP-ASIC showed SEEs which required power cycling of the components to recover their functionality. The SEE affecting the DSP-ASIC also increased the post forward error correction bit error ratio (BER), but the BER nevertheless remained sufficiently low in practice. These radiation test results show that these COTS components can be good candidates for use in satellite communications.

Keywords: optical communication, satellite communication, digital coherent, proton radiation

1. INTRODUCTION

Optical satellite communications technologies for throughputs from 100 Gb/s to Tb/s levels are under development, and digital coherent detection and wavelength division multiplexing (WDM), which are widely used in commercial optical fiber communications, are promising technologies for this purpose [1-3]. The adoption of these technologies leads to the possibility of using high performance, low cost commercial off the shelf (COTS) components [4], such as various optical devices and digital signal processing (DSP) application specific integrated circuits (ASIC), in satellite communication terminals (CTs). However, the evaluation and screening of such components for use in the space environment is necessary [5]. Evaluations of COTS optical devices operating with signals at more than 100 Gb/s have not been reported, and few evaluations of COTS DSP-ASICs have been reported for proton radiation [6, 7] and heavy ion radiation [8]. In [6] and [7], DSP-ASICs were exposed to proton streams, but the impact of the single event effect (SEE) on bit error ratio (BER) was not reported.

In this paper, we present the evaluation of COTS optical devices and a DSP-ASIC suitable for enabling 100 Gb/s/wavelength capacity when subjected to proton radiation testing. The COTS optical devices and the DSP-ASIC were successively exposed to 70 MeV protons, and the impacts of SEE and total non-ionizing dose (TNID) / total ionizing dose (TID) on the BER were evaluated using 100 Gb/s signals.

2. DIGITAL COHERENT TECHNOLOGY FOR OPTICAL SATELLITE COMMUNICATIONS

Figure 1 shows the configuration of the typical optical satellite communication system with digital coherent technology considered in this paper. Two satellites have the same CTs and communicate in both directions with wavelength division

*Matsuda.Keisuke@db.MitsubishiElectric.co.jp

multiplexed 100 Gb/s dual polarization quadrature phase shift keying (DP-QPSK) signals. In the CTs, the 100 Gb/s DP-QPSK signals are transmitted and received using 100 Gb/s digital coherent transceivers (TRx) on different wavelengths, each carrying 10 x 10 Gb/s of payload data. The transmit signals are wavelength multiplexed at the optical wavelength multiplexer (MUX) and transmitted to free space through the telescope. The signals received through the telescope are wavelength demultiplexed at the optical wavelength demultiplexer (Demux) and processed in the 100 Gb/s digital coherent TRxs.

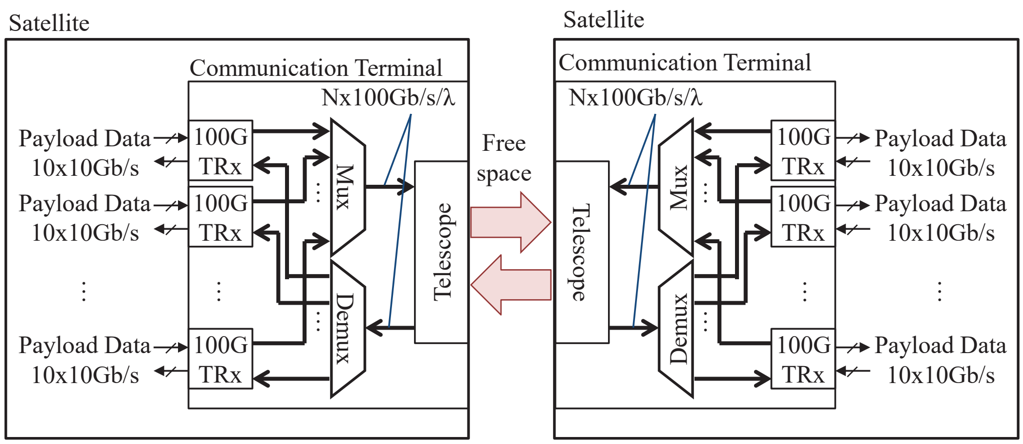

Figure 1. Configuration of Optical Satellite CT

The 100 Gb/s digital coherent TRx evaluated in this work is shown in Figure 2. 10 x 10 Gb/s data are forward error correction (FEC) coded, framed and mapped to the DP-QPSK signals in the DSP-ASIC. The light from the micro integrable tunable laser assembly (Micro ITLA) [9] is modulated by the lithium niobate (LN) modulator [10] with the DP-QPSK signals from the DSP-ASIC via the modulator drivers. The output power is monitored by delivering a part of the light to the photodiode (PD). The received signals are coherently detected with the light from another Micro ITLA at the micro intradyne coherent receiver (Micro ICR) [11] and demodulated at the DSP-ASIC. The demodulated signals are FEC decoded and converted to 10 x 10 Gb/s data. In this work we evaluated a transmitter Micro ITLA, a LN modulator, a Micro ICR and a DSP-ASIC.

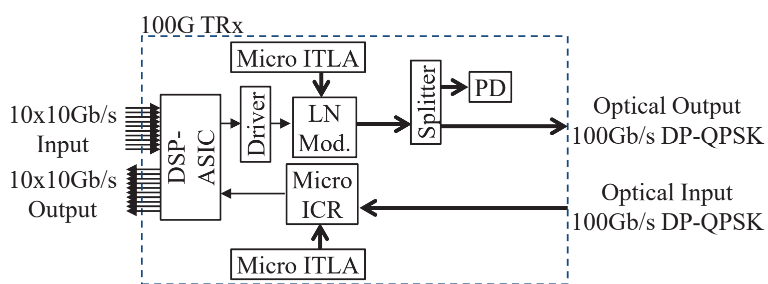

Figure 2. 100 Gb/s Digital Coherent Transceiver

3. EXPERIMENTS

3.1 Performance measurement setup

We used two different setups for measuring the performance of the 100 Gb/s signal. For testing the Micro ITLA and LN modulator, we used the setup shown in Figure 3, and for testing the DSP-ASIC and Micro ICR, we used the setup shown in Figure 4. In the Figure 3 setup, we used two TRxs. One is used as the transmitter and the other is used as the receiver.

Between the transmitter and the receiver, amplified spontaneous emission (ASE) noise is added to the signals. We irradiated the Micro ITLA used as the light source for the transmit signal and the LN modulator in the transmitter with protons. The pre-FEC bit error ratio (BER) of the 100 Gb/s signal was measured. In the Figure 4 setup, we used a single TRx. The optical output is returned to the same TRx after ASE noise is added. The pre-FEC BER of the 100 Gb/s signal was measured, and one of the 10 Gb/s signals was monitored with a small form-factor pluggable plus (SFP+) module and a synchronous digital hierarchy (SDH) analyzer. At the SDH analyzer we measured the post-FEC BER and monitored the SDH alarms.

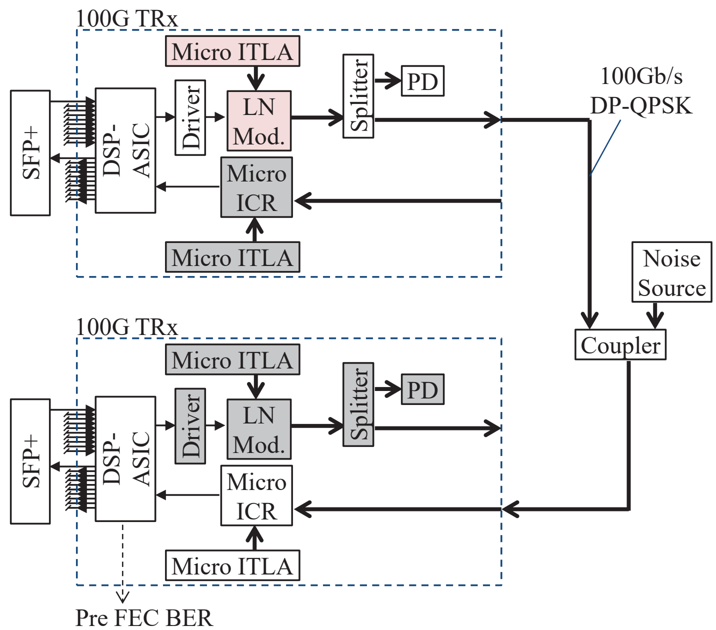

Figure 3. Performance measurement setup for the Micro ITLA and LN Modulator

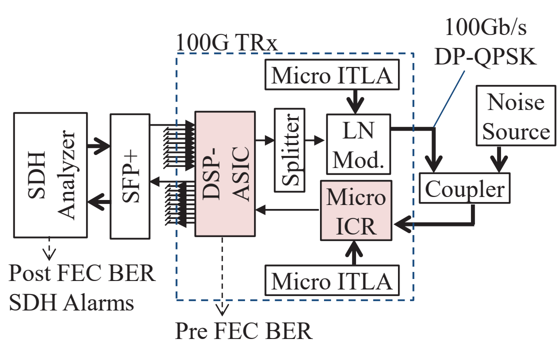

Figure 4. Performance measurement setup for the Micro ICR and DSP-ASIC

3.2 Test of Micro ITLA

The Micro ITLA consists of a laser diode chip mounted in a ceramic package and a printed circuit board which controls the chip. The ceramic package was irradiated with protons 6 times. Details of the irradiation conditions are shown in Table

1. The energy of the protons was set to 70 MeV. The ASE noise level was adjusted so that the Q margin above the FEC threshold was 2.2 dB before irradiation. The Q margin was calculated from the pre-FEC BER.

Throughout Tests No. 1 to No. 6, the Q margin showed no degradation and no SEE was observed. Also, the monitored output optical power did not change. Figure 5 shows the time variation of the Q margin during Test No. 6 as an example. The irradiation duration was 500 seconds as indicated in Figure 5. No degradation is observed in Figure 5. Figure 6 shows the transmitted optical spectrum before and after the irradiation test of the Micro ITLA. The spectra show that the wavelength of the output of the Micro ITLA was not affected by the irradiation.

Table 1. Proton irradiation test conditions for Micro ITLA

Test No.	Average Flux [p/cm^2/s]	Time Duration [s]	Cumulative Fluence [p/cm^2]	Cumulative TID [krad(Si)]	Q margin before irradiation
1	2×10^7	300	6×10^9	1	2.2 dB
2	2×10^8	166	2.6×10^{10}	3	
3	2×10^8	400	1.1×10^{11}	13	
4	2×10^8	500	2.1×10^{11}	25	
5	2×10^8	500	3.1×10^{11}	36	
6	2×10^8	500	4.1×10^{11}	48	

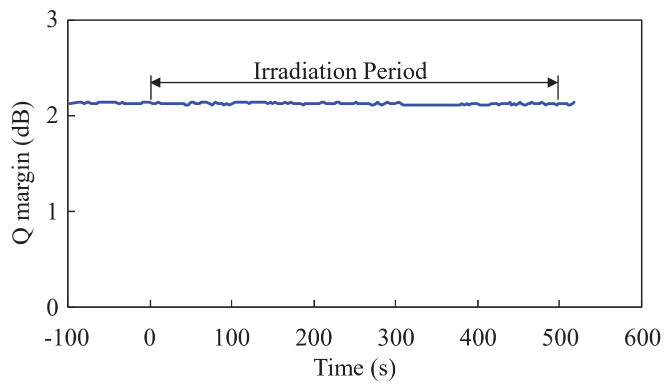

Figure 5. Q margin variation during Test No. 6

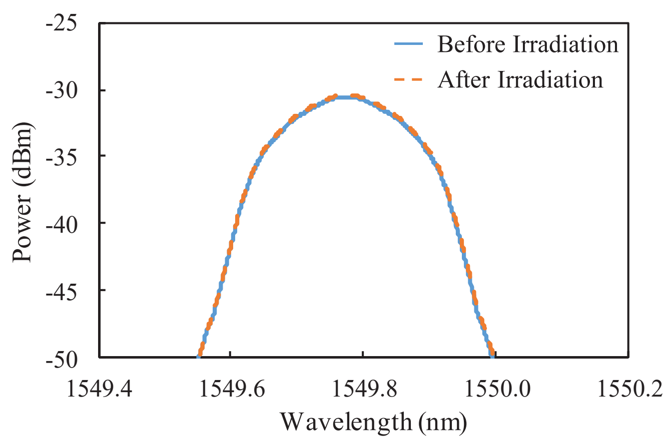

Figure 6. Spectrum of the transmitted signal before and after the irradiation of the micro ITLA

3.3 Test of LN modulator

The LN modulator uses 4 Mach-Zehnder modulators for phase modulation. The area of the traveling-wave electrodes of the Mach-Zehnder modulators was irradiated with protons twice. Details of the irradiation conditions are shown in Table 2. The energy of the protons was set to 70 MeV. The ASE noise level was adjusted so that the Q margin above the FEC threshold was about 2.2 dB before irradiation.

Throughout Tests No. 7 and No. 8, the Q margin showed no degradation and no SEE was observed. Also, the monitored output optical power did not change. Figure 7 shows the time variation of the Q margin during Test No. 8 as an example. The irradiation duration was 800 seconds as indicated in Figure 7. No degradation is observed in Figure 7. Figure 8 shows the transmitted optical spectrum before and after the irradiation test of the LN modulator. The modulated spectrum is not affected by the irradiation.

Table 2. Proton irradiation test conditions for LN Modulator

Test No.	Average Flux [p/cm^2/s]	Time Duration [s]	Cumulative Fluence [p/cm^2]	Cumulative TID [krad(Si)]	Q margin before irradiation
7	2x10^8	500	9.9x10^{10}	1	2.2 dB Q Margin
8	2x10^8	800	2.7x10^{11}	3	

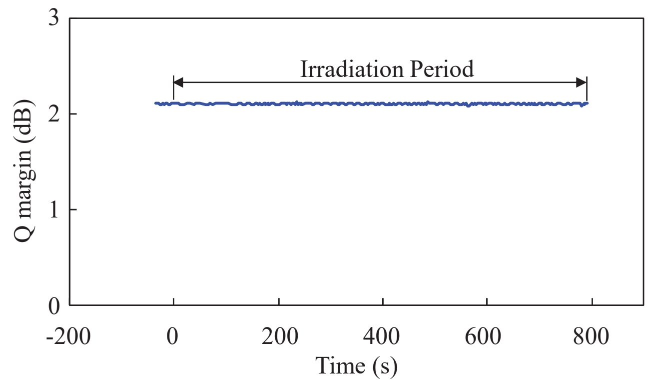

Figure 7. Q margin variation during Test No. 8

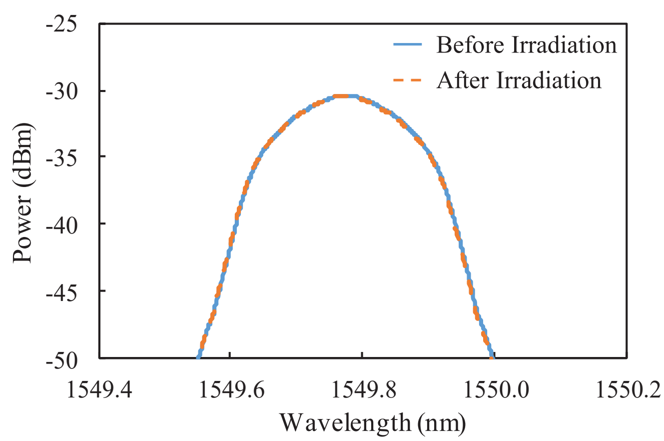

Figure 8. Spectrum of the transmitted signal before and after the irradiation of the LN modulator

3.4 Test of DSP-ASIC

The DSP-ASIC tested in this work uses 20 nm complementary metal oxide semiconductor technology, and it includes a digital to analog converter and analog to digital converter working at 64 G samples per second. The package is a ball grid array type. We cooled the package from the top by air cooling without any heat sink, and the protons were applied from the same side. The DSP-ASIC was irradiated with protons three times. Details of the irradiation conditions are shown in Table 3. The energy of the protons was set to 70 MeV. For the test of the DSP-ASIC the noise loading was stopped, so that any slight increase of the BER due to SEE could be monitored.

Table 3. Proton irradiation test conditions for the DSP-ASIC

Test No.	Average Flux [p/cm^2/s]	Time Duration [s]	Cumulative Fluence [p/cm^2]	Cumulative TID [krad(Si)]
9	$1x10^8$	423	$4.3x10^{10}$	5
10	$1.5x10^7$	500	$5.0x10^{10}$	6
11	$5.3x10^7$	100	$1.0x10^{11}$	11

Figure 9 and Figure 10 show the pre-FEC BER, post-FEC BER, SDH out of frame alarms (OOF), and SDH loss of frame alarms (LOF) monitored before the irradiation test and during irradiation testing of the DSP-ASIC. The irradiation periods are indicated in Figure 10. As seen in Figure 9, no post-FEC errors or SDH alarms were observed in the absence of irradiation.

Figure 10 (a) shows the results for the highest average flux. In Figure 10 (a), increases in the pre-FEC BER and the number of SDH alarms were observed due to the irradiation. After 250 s, the pre-FEC BER showed a continuously high BER, and after 420 s continuous SDH LOF was observed. Subsequent power cycling restored the functionality of the DSP-ASIC.

The increases in the pre-FEC BER and number of SDH alarms were caused by errors in the equalization of the signal due to SEEs in the equalization circuit. The continuously high BER was caused either by errors in the equalization parameters or by the convergence of the adaptive equalization to an undesirable local minimum. Since SDH OOFs were observed when the pre-FEC BER did not show any degradation, the alarms were caused either by errors in the FEC decoding or in subsequent stages of the DSP-ASIC. At 129 s and 277 s, pre-FEC BER increases caused SDH LOF.

Figure 10 (b) and (c) show the results of Tests No. 10 and No. 11 with lower average flux levels than in Test No. 9. The Pre-FEC BER increases were less than in Test No. 9, but SDH OOF and SDH LOF were still observed as in the case of Test No. 9.

Figure 11 shows the transmitted optical spectrum before and after the irradiation test of the DSP-ASIC. The modulated spectrum is not affected by the radiation. This means that there was no degradation of the DAC in the DPS-ASIC. The effects on BER performance in a noise loading test were evaluated after irradiation of the Micro ICR.

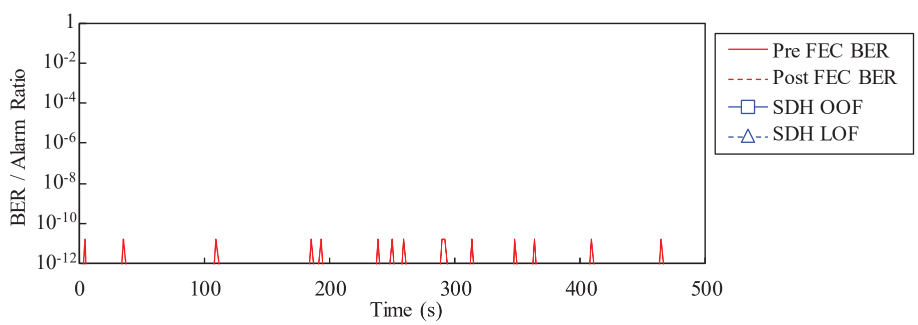

Figure 9. Monitored BER and alarms without irradiation

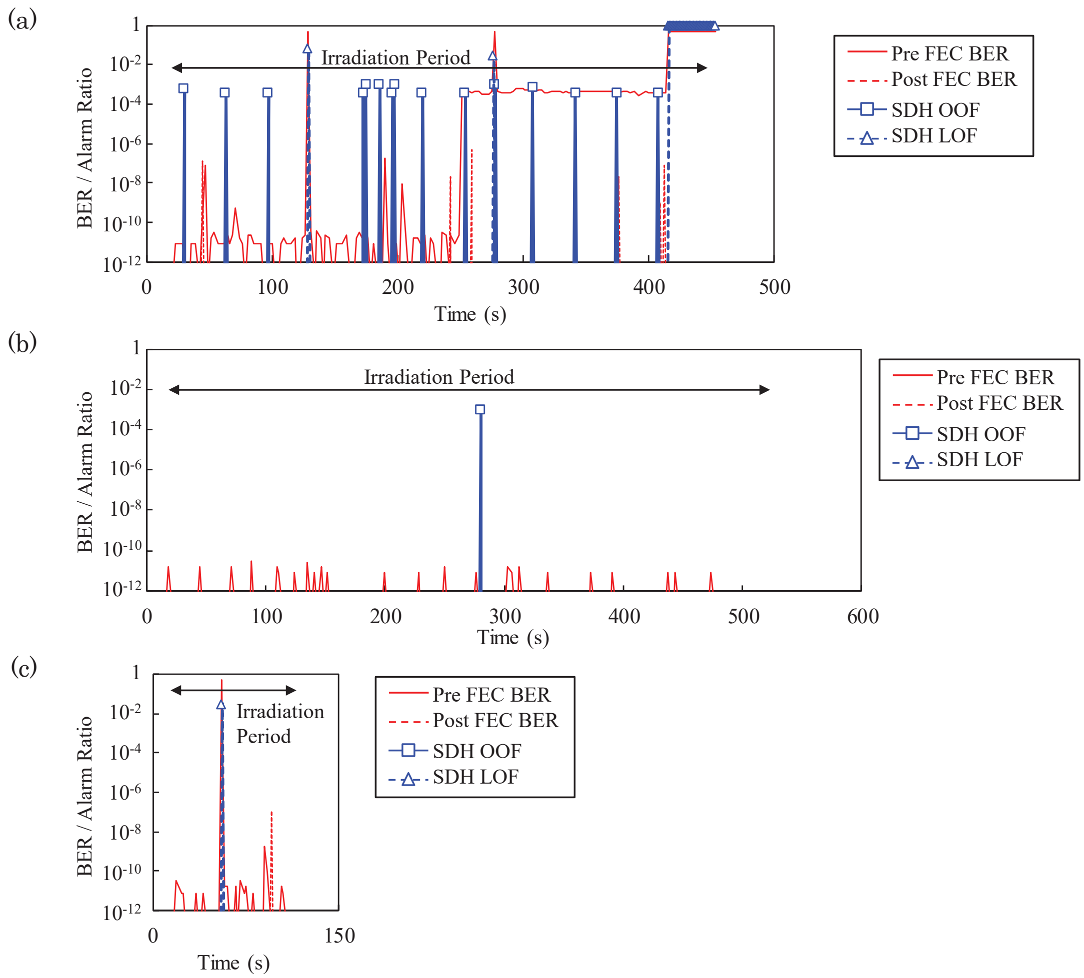

Figure 10. Monitored BER and alarms during the testing of the DSP-ASIC: (a) Test No. 9, (b) Test No. 10 and (c) Test No. 11.

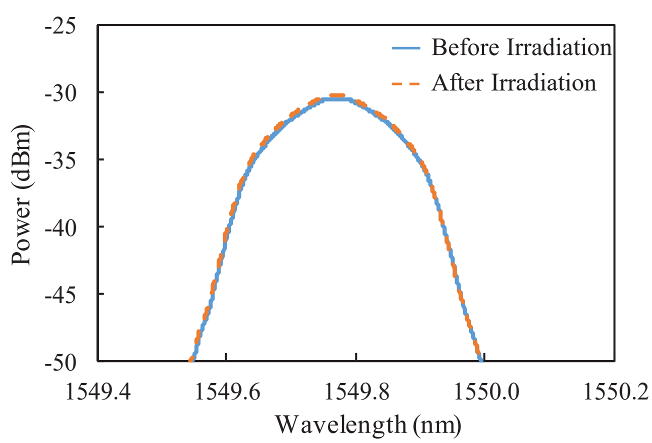

Figure 11. Spectrum of the transmitted signal before and after the irradiation of the DSP-ASIC

3.5 Test of Micro ICR

The Micro ICR consists of an interferometer, 4 PDs and 4 transimpedance amplifiers (TIA), in a ceramic package. The gain of the TIAs is controlled within the Micro ICR to keep the output amplitude constant. The area of the PDs and TIAs was irradiated with protons twice. Details of the irradiation conditions are shown in Table 4. The energy of the protons was set to 70 MeV. In Test No. 12, the noise loading was stopped, and in Test No. 13 the ASE noise level was adjusted so that the Q margin above the FEC threshold was about 2.0 dB before irradiation.

Table 4. Proton irradiation test conditions for the Micro ICR

Test No.	Average Flux [p/cm^2/s]	Time Duration [s]	Cumulative Fluence [p/cm^2]	Cumulative TID [krad(Si)]	Q margin before irradiation
12	2.2x10^8	100	2.2x10^{10}	3	>15 dB (without noise loading)
13	2.2x10^8	500	1.3x10^{11}	25	2.0 dB

Figure 12 shows the BER and SDH alarms monitored during Test No. 12. The irradiation duration was 100 seconds as indicated in Figure 12. The Pre-FEC BER did not show any significant increase, but SDH OOF was observed. Since the DSP-ASIC was located near the Micro ICR, collateral irradiation caused SEE in the DSP-ASIC.

Figure 13 shows the Q margin, post-FEC BER and SDH alarms monitored during Test No. 13. The irradiation duration was 500 seconds as indicated in Figure 13. Before 175 s, SDH OOF was observed with no degradation of the Q margin. This was caused by SEE in the DSP-ASIC as in the case of Test No. 12. After 175 s, continuous SDH LOF was observed. We observed that the output level of the Micro ICR monitored in the DSP-ASIC was less than 1% of that before irradiation. This was caused by SEE in the gain control circuits of the TIAs. Subsequent power cycling restored the output level of the Micro ICR.

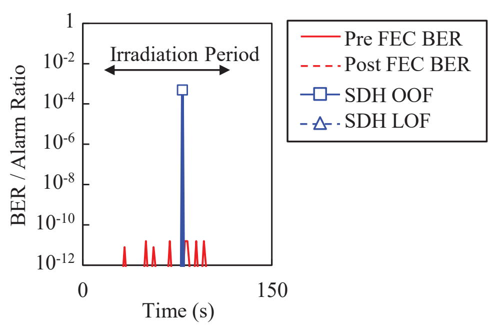

Figure 12. Monitored BER and SDH alarms in the test of the Micro ICR (Test No. 12).

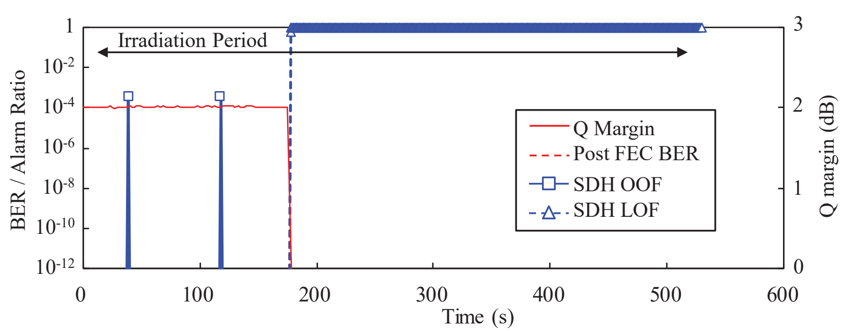

Figure 13. Monitored BER and SDH alarms in the test of the Micro ICR (Test No. 13).

After the irradiation of the DSP ASIC and the Micro ICR, the Q margin calculated from the pre-FEC BER in the noise loading test was measured and compared with that before the irradiation. Figure 14 shows the results of the noise loading tests. No degradation due to the TNID/TID effect was observed.

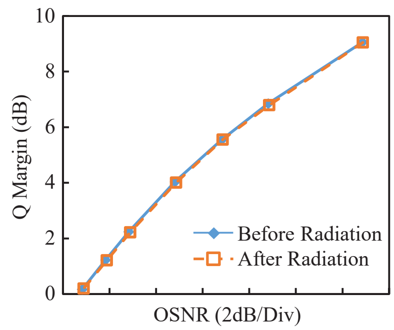

Figure 14. Measured noise loading test Q margin before and after irradiation of the DSP-ASIC and Micro ICR

4. DISCUSSION

In this work, as COTS components of a 100 Gb/s Digital Coherent TRx, a Micro ITLA, a LN modulator, a Micro ICR and a DSP-ASIC were exposed to a total fluence of 70 MeV protons of more than 4.1×10^{10} p/cm^2. This fluence is equivalent to the TNID/TID experienced during 10 years in low earth orbit. All components showed no degradation as a result of TNID/TID effects.

On the other hand, the Micro ICR and DSP-ASIC showed SEEs from which they did not recover autonomously, but power cycling restored their functionality. Therefore, if this DSP-ASIC and Micro ICR are to be adopted in satellite CTs, an external function to reset the components would be necessary to recover from severe SSEs. Single events in the DSP-ASIC also caused an increase in the post-FEC BER. In the most severe test, No. 9, the average post-FEC BER was 5.97×10^{-5}. Considering that the proton flux in the test was 3×10^{5} times higher than in the real space environment, any BER increase due to SEE is expected to be sufficiently low in practice.

5. CONCLUSIONS

The COTS optical devices and the DSP-ASIC of a 100 Gb/s digital coherent TRx were evaluated when subjected to proton radiation testing. The proton irradiation of the test is equivalent to the TNID/TID experienced during 10 years in low earth orbit. All the optical devices and the DSP-ASIC showed no degradation from TNID/TID effects. Any Post FEC BER increase due to SEEs in the DSP-ASIC were sufficiently low in practice, but severe SEEs in the DSP-ASIC and Micro ICR did require power cycling. These results showed that these COTS components can be good candidates for use in satellite communications.

REFERENCES

[1] T. Araki, "A study of the future optical data relay system; requirements, problems and solution," *Proc. International Conference on Space Optical Systems and Applications (ICSOS) 2017*, pp. 199-202.

[2] R. M. Calvo, J. Poliak, J. Surof, A. Reeves, M. Richerzhagen, H. F. Kelemu, R. Barrios, C. Carrizo, R. Wolf, F. Rein, A. Dochhan, K. Saucke, W. Luetke, "Optical technologies for very high throughput satellite communications," *Proc. SPIE* 109100W (2018).

[3] K. Matsuda, S. Koshikawa, T. Yoshida and N. Suzuki, "Fiber Coupling Loss Mitigation of Wavelength Division Multiplexed 20 Gb/s QPSK Signal with 3-Mode Fiber," Proc. *International Conference on Space Optical Systems and Applications (ICSOS) 2019*, S2.3.

[4] B. S. Robinson, D. M. Boroson, C. M. Schieler, F. I. Khatri, O. Guldner, S. Constantine, T. Shih, J. W. Burnside, B. C. Bilyeu, F. Hakimi, A. Garg, G. Allen, E. Clements, D. M. Cornwell, "TeraByte InfraRed Delivery (TBIRD): a demonstration of large-volume direct-to-Earth data transfer from low-Earth orbit," *Proc. SPIE* 105240V (2018).
[5] J. Nakamura, H. Kotake, T. Goda, Y. Hashimoto, Y. Oshima, "Study on a screening test process for quality assurance of optical communication devices for satellite," *Proc. SPIE* 109101M (2019).
[6] R. J. Aniceto, S. Moro, R. Milanowski, C. Isabelle, N. Hall, B. Vermeire, K. Cahoy, "Single Event Effect and Total Ionizing Dose Assessment of Commercial Optical Coherent DSP ASIC," *Proc. 2017 Radiation Effects Data Workshop (REDW)*, pp. 231-236.
[7] R. J. Aniceto, S. Moro, A. Grier, R. Milanowski, K. Cahoy, "Assessment of gamma and proton radiation effects on 100 Gbps commercial coherent optical transceiver," *Proc. SPIE* 111805U, (2018).
[8] R. J. Aniceto, R. Milanowski, S. McClure, A. Aguilar, S. Moro, E. D. Miller, K. Cahoy, N. Nicholson, D. Greene, "Heavy Ion radiation assessment of a 100G/200G commercial optical coherent DSP ASIC," *Proc. SPIE* 1091011 (2019).
[9] OIF Implementation Agreement, "Micro Integrable Tunable Laser Assembly Implementation Agreement," OIF-MicroITLA-01.1, (2015).
[10] OIF Implementation Agreement, "Implementation Agreement for Integrated Polarization Multiplexed Quadrature Modulated Transmitters," OIF-PMQ-TX-01.2, (2015).
[11] OIF Implementation Agreement, "Implementation Agreement for Micro Intradyne Coherent Receivers," OIF-DPC-MRX-02.0, (2017).